

# HORIZONTAL COUPLING IMPEDANCE OF THE APS STORAGE RING\*

Yong-Chul Chae<sup>†</sup>, Katherine Harkay, Xiang Sun

Advanced Photon Source, Argonne National Laboratory, Argonne, IL 60439 USA

## Abstract

The three-dimensional wake potentials of the APS storage ring have been reconstructed according to the impedance database concept. Every wakefield-generating component in the ring was considered including small-gap insertion device (ID) chambers, rf cavities, shielded bellows, beam position monitors, synchrotron radiation absorbers, scrapers, flags, various chamber transitions, septum chambers, and pulsed kickers. In this paper the result for the horizontal wake potentials and its impedance are presented. The numerically obtained impedance has been used to investigate the experimental results. Tune shift was calculated and compared with the measurement. We also observed a horizontal focusing in the calculated wake potential of the shallow transition without rotational symmetry.

## IMPEDANCE DATABASE

The concept of impedance database is described in the companion paper [1]. We report highlights of building the database for the horizontal impedance. The longitudinal and vertical impedance are reported separately [2,3].

### Insertion Device

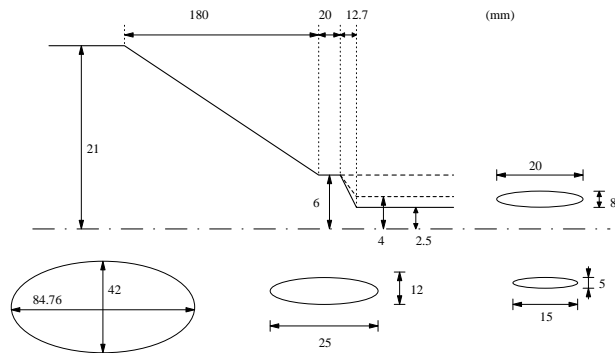


Figure 1: Transition between regular and ID chambers.

At the APS, the vacuum chamber for an insertion device is 5 m long with a small gap; its schematic diagram is shown in Fig. 1, which shows the transition from the regular chamber (8.4 cm by 4.2 cm) to the small-gap chambers whose vertical dimensions are 5 mm or 8 mm. There are 22 chambers with 8-mm gap and 2 chambers with 5-mm gap installed in the storage ring (there are no longer any 12-mm chambers).

The ID chambers have a detrimental effect on the single-bunch current limit in the vertical plane due to beam-chamber interaction. However its horizontal effects

seemed to be small and were not well known.

We used the program MAFIA in order to calculate the wake potential for a bunch of 5 mm. The simulation conditions are described in detail in the companion papers [1,3]. The results show that the horizontal wake is 100 times smaller than the vertical wake.

The smallness of the horizontal wake was found to be due to the cancellation between the wakes obtained by two different boundary conditions imposed on the symmetry plane. The electric boundary condition is  $E=0$  (E-wake), and the magnetic boundary condition is  $H=0$  (H-wake). The two wake potentials, E-wake and H-wake, shown in Fig. 2, were found to be opposite in the sign but nearly equal in magnitude. Therefore, the total horizontal wake, which is  $(E\text{-wake} + H\text{-wake})/2$ , becomes small.

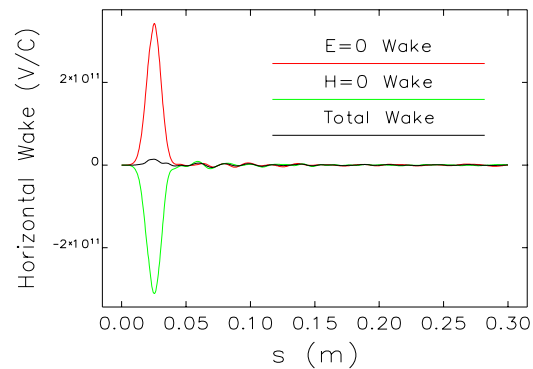


Figure 2: Total horizontal wake is the sum of E-wake and H-wake.

### Beam Position Monitor (BPM)

Two main types of BPMs are installed in the ring: 1) 400 BPMs with standard buttons installed at the regular chambers, and 2) 24 BPMs with mini-buttons installed at the ID chambers. These are called the P0-BPMs. We will show later that these BPMs contribute the most to total horizontal impedance. The P0-BPM has an especially strong influence on the beam because of its proximity to the beam.

The geometry of the P0-BPM used in the MAFIA simulation is shown in Fig. 3. The long coaxial conductor above the button characterizes a large resonance peak at 22 GHz in the total impedance.

The results from MAFIA simulation are shown in Fig. 4. The top graph shows the long-ranged wake modulated by the 22 GHz wavelength. The impedance is shown in the bottom graph and exhibits a few resonant peaks.

\* Work supported by the U.S. Department of Energy, Office of Basic Energy Sciences under Contract No. W-31-109-ENG-38.

<sup>†</sup> chae@aps.anl.gov

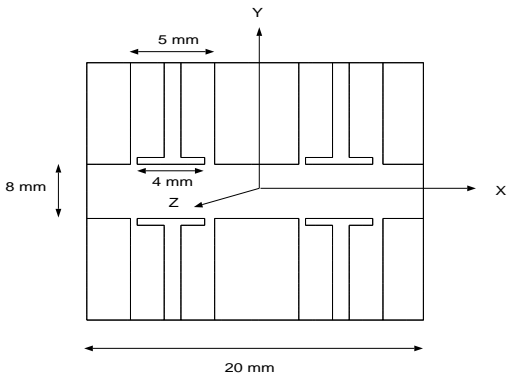


Figure 3: P0-BPM geometry used in the MAFIA simulation.

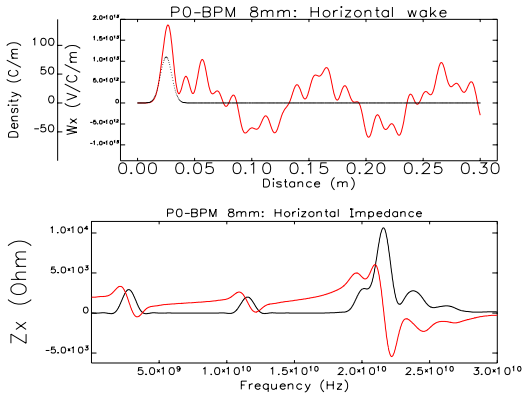


Figure 4: P0-BPM's wake (top); its impedance (bottom).

**Bellow (Focusing Wake Potential)**

The bellows in the APS storage ring are shielded by sliding contacts. Figure 5 is a drawing of the B1 bellow, one of six different types of bellows. The transition in the horizontal dimension varies from 8.4 cm to 9.3 cm, giving a transition angle of 4 deg. The transition angle in the vertical dimension is slightly greater, varying from 4.07 cm to 5.39 cm, giving 5.7 deg.

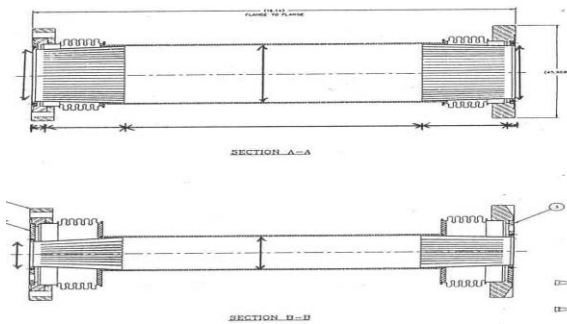


Figure 5: Drawing of the B1-bellow: horizontal plane (top), vertical plane (bottom).

The results from the initial simulation by MAFIA showed a slightly negative kick factor; this implies that the bunch traversing the bellows would receive a focusing kick instead of a defocusing kick. The longitudinal equivalent of this phenomenon would be gaining energy

instead of losing energy by the beam. The small magnitude of wake potential, as well as the negative sign, was unexpected. In order to verify the simulation result, we carried out a series of phenomenological investigations to study the mesh effect, bunch-length effect, 2-D simplification, angle effect, etc. The results from a systematic case study of the transition geometry is presented below.

We devised the structure similar to the bellows depicted in Fig. 5. The cross section is an ellipse whose taper and aspect ratio are varied. The semimajor axis is varied from 2 cm to one of 2, 2.25, 2.5, 2.75, or 3.0 cm and back to 2 cm. The tapering of the semiminor axis is not varied; tapering is from 1 cm to 1.3 cm and back to 1.0 cm. The semimajor axis in the middle section,  $a_m$ , identifies each case.

A half chamber is used in the simulation with two boundary conditions, E-wake and H-wake. The total wakes, the E-wakes, and the H-wakes are shown in Fig. 6. Each case for the different value of  $a_m$  is represented by a different curve. From the E-wake plot, we observe that the sign of the wake is always positive, and its magnitude decreases as the variation of the aperture is reduced. However, from the H-wake plot, we clearly see that the sign changes; a transition occurs at  $a_m=2.5$  cm, and the wake becomes more negative as  $a_m$  is further reduced. The total wake, then, eventually becomes negative at  $a_m=2.0$  cm. Transition from positive to negative occurs for the total wake at  $a_m=2.25$  cm.

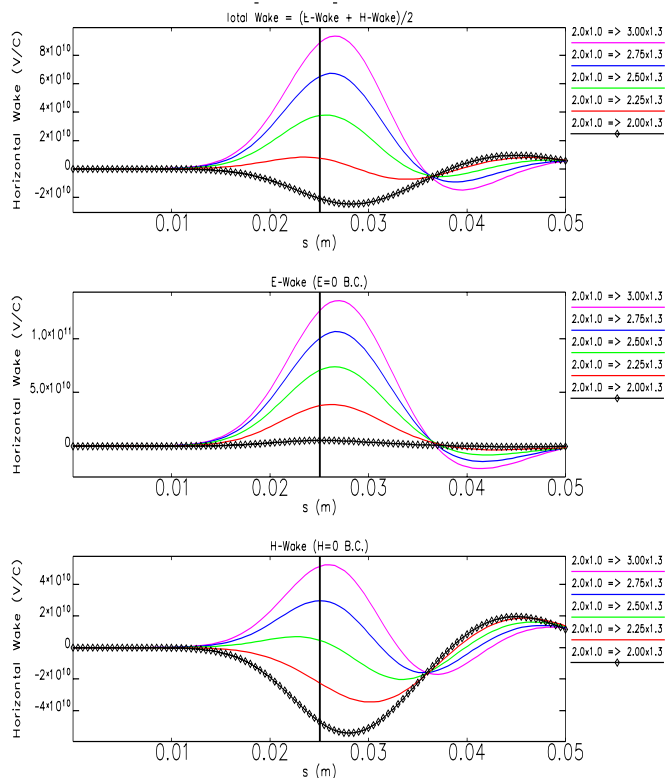


Figure 6: Horizontal wake potentials of 3-D elliptical taper: total wake (top), electric boundary condition (middle), magnetic boundary condition (bottom).

Based on the above study we conjecture that:

- 1) the negative wake potential is a completely three-dimensional phenomena,
- 2) it can occur when the degree of perturbation in one dimension is greater than in the other,
- 3) the negative wake potential is in the plane of the smaller perturbation.

In our bellows example, the smaller perturbation is in the horizontal plane where the negative wake occurred.

### TOTAL IMPEDANCE

The total wake potential for the bunch of 5 mm and the impedance derived from it are shown in Fig. 7. The shape of the wake potential follows the charge profile at the head but is distorted near the tail and then followed by an extended wake. The impedance at low frequency is about 0.22 MΩ/m; the previous estimate based on the tune slope measurement also predicted a similar result [4]. A broadband resonator (BBR) was used to model the impedance; its parameters were found to be shunt impedance  $R_s=0.6$  MΩ, quality factor  $Q=4$ , and resonant frequency  $f_r=22$  GHz.

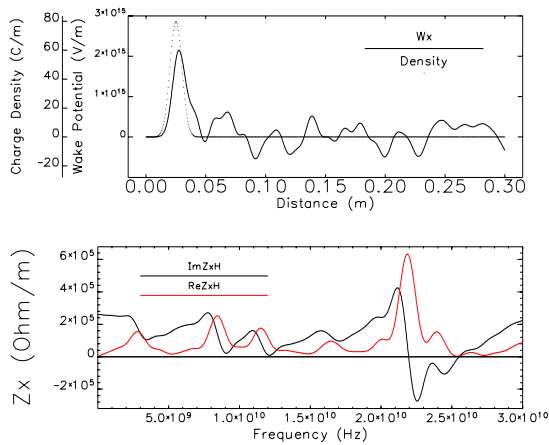


Figure 7: Horizontal wake potential and impedance of the ring

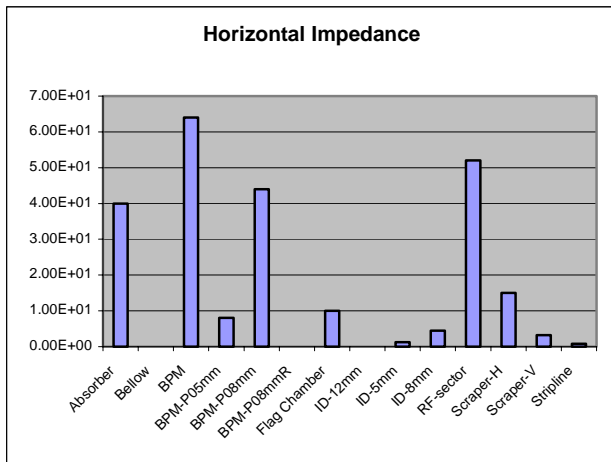


Figure 8: Horizontal impedance breakdown.

The breakdown of total impedance is presented in Fig. 8. From the figure we identify the major contributors, which are the BPM, P0-BPM, rf sector, and synchrotron radiation absorber.

### APPLICATION

We used the total impedance in order to investigate the current-dependent beam dynamics observed in the ring. We chose the tune slope to compare. The recently measured value was  $8 \times 10^{-4}/\text{mA}$ , which was fitting tune shifts over the current from 2 mA to 10 mA [4,5].

The numerical estimate is based on the well-known formula:

$$\frac{dv}{dI} = \frac{R}{2\pi\sigma_s E/e} \sum_{Elements} \beta_i Z_{eff}$$

where  $\beta_i$  is the betatron function at the location of the impedance element. Note that the tune slope depends on the bunch length and chromaticity.

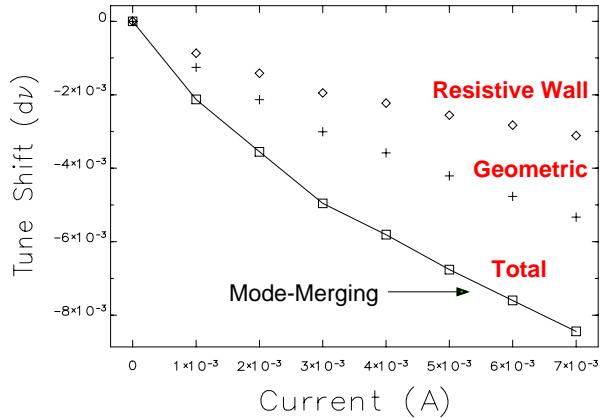


Figure 9: Tune slope as function of chromaticity for the 2.5-nm lattice.

The resultant tune shift as a function of current is shown in Fig. 9. We used the impedance shown in Fig. 7 and incorporated the measured bunch lengths (42 ps at 5 mA, for example) in the calculation. The tune slope, by fitting over 2 mA to 7 mA, is  $9 \times 10^{-4}/\text{mA}$ , which is slightly larger than the measured value. The horizontal tune is reduced by the amount of synchrotron tune,  $v_s=0.007$ , at the current 5.5 mA, which is close to mode-merging current observed in the ring. Contrary to results in the vertical plane, the resistive-wall impedance constitutes 1/3 of the total in the horizontal plane, so that its effect is expected to be dominant. An investigation is under way.

### REFERENCES

- [1] Y.-C. Chae, "The impedance database and its application to the APS storage ring," these proceedings.
- [2] Y.-C. Chae et al., "Longitudinal coupling impedance of the APS storage ring," these proceedings.
- [3] Y.-C. Chae et al., "Vertical coupling impedance of the APS storage ring," these proceedings.
- [4] K.C. Harkay et al., *Proc. 1999 PAC*, 1644 (1999).
- [5] V. Sajaev, private communication.